Supplement of Atmos. Meas. Tech., 17, 755–764, 2024
https://doi.org/10.5194/amt-17-755-2024-supplement

Atmospheric Measurement Techniques
Open Access
EGU

Supplement of

Wall loss of semi-volatile organic compounds in a Teflon bag chamber for the temperature range of 262–298 K: mechanistic insight on temperature dependence

Longkun He et al.

Correspondence to: Mikinori Kuwata (kuwata@pku.edu.cn) and Yingjun Liu (yingjun.liu@pku.edu.cn)

Table S1. List of n-alkanes used for the present study, along with the saturation vapor pressure at 298 K predicted by the EVAPORATION group contribution method (Compernolle et al., 2011). All the chemicals were purchased from Konoscience.

compound name	carbon number	CAS number	purity	saturation vapor pressure (Pa)
n-tetradecane	14	629-59-4	99%	2.8E+00
n-pentadecane	15	629-62-9	98%	9.2E-01
n-hexadecane	16	544-76-3	98%	3.0E-01
n-heptadecane	17	629-78-7	99%	1.0E-01
n-octadecane	18	593-45-3	99%	3.3E-02
n-nonadecane	19	629-92-5	98%	1.1E-02

Table S2. Abundances of diisobutyl phthalate (DiBP) and dibutyl phthalate (DnBP) in and outside of the chamber (*i.e.*, room air in the laboratory) detected by the SV-TAG during one experiment at room temperature.[a]

time after injection (min)	peak area (counts)[b]		ratio of chamber air to room air	
	DiBP	DnBP	DiBP	DnBP
chamber background (0)	15618	12532	0.44%	0.47%
73	16197	15266	0.46%	0.57%
133	19457	24483	0.55%	0.91%
206	18029	20958	0.51%	0.78%
406	18920	21996	0.53%	0.82%
553	13110	13526	0.37%	0.50%
733	13073	11923	0.37%	0.45%
936	14189	12866	0.40%	0.48%
Reference value for the room air	3539783	2679338	-	-

[a] DiBP and DnBP were selected, as they were abundant in the room air of the laboratory. The consistently low concentration in the chamber bag suggested that intrusion of the room air into the experimental setup was minimal.

[b] Peak areas were integrated by Agilent MassHunter Station Quantitative Analysis (10.0, Agilent Technologies, Inc.).

Table S3. Fitting and measurement results for room-temperature experiments.

Compound	Experiment shown in Figure 3[a]			All three room-temperature experiments[b]		
	k_1 (s^{-1})	k_{-1} (s^{-1})	k_2 (s^{-1})[c]	K_{eq}	$1/[C_{gas}/C_0]_{\text{at 3 hours}} - 1$	relative difference
C_{14} *n*-alkane	2.76×10^{-4}	2.07×10^{-4}	9.39×10^{-6}	1.00 ± 0.27	1.14 ± 0.23	16% ± 8%
C_{15} *n*-alkane	2.79×10^{-4}	2.07×10^{-4}	1.87×10^{-5}	1.08 ± 0.19	1.23 ± 0.21	13% ± 6%
C_{16} *n*-alkane	3.41×10^{-4}	1.84×10^{-4}	2.67×10^{-5}	1.72 ± 0.17	1.98 ± 0.14	16% ± 11%
C_{17} *n*-alkane	4.63×10^{-4}	1.82×10^{-4}	3.60×10^{-5}	2.73 ± 0.50	3.27 ± 0.15	23% ± 16%
C_{18} *n*-alkane	6.35×10^{-4}	2.13×10^{-4}	4.35×10^{-5}	3.91 ± 1.27	4.85 ± 0.57	31% ± 23%
C_{19} *n*-alkane	1.17×10^{-3}	2.25×10^{-4}	4.62×10^{-5}	8.69 ± 4.37	10.53 ± 2.80	35% ± 27%

[a] Optimized parameter sets of the two-layer model used in Figure 3. Best-fit parameters were obtained by the Newton method via Wolfram Mathematica 13.1.

[b] (Mean value) ± (standard deviation) are presented.

[c] k_2 obtained here was not used in Section 3.3 (characterization of diffusion in the Teflon wall). These fittings overestimated the first-order loss rate constant for low volatile species, C_{16} – C_{19} *n*-alkanes, as shown in Figure 3.

Table S4. List of investigated chemical species by each study in Figure 6.

Source	chemical species
This work	*n*-alkanes
Yeh and Ziemann (2015)	2-ketones, 2-alcohols, monoacids, and 1,2-diols
Matsunaga and Ziemann (2010)	*n*-alkanes and 1-alkenes
Yeh and Ziemann (2014)	alkylnitrates
Krechmer et al. (2016)	dihydroxynitrates (DHNs), dihydroxycarbonylnitrates (DHCNs), and tri-hydroxynitrates (THNs)

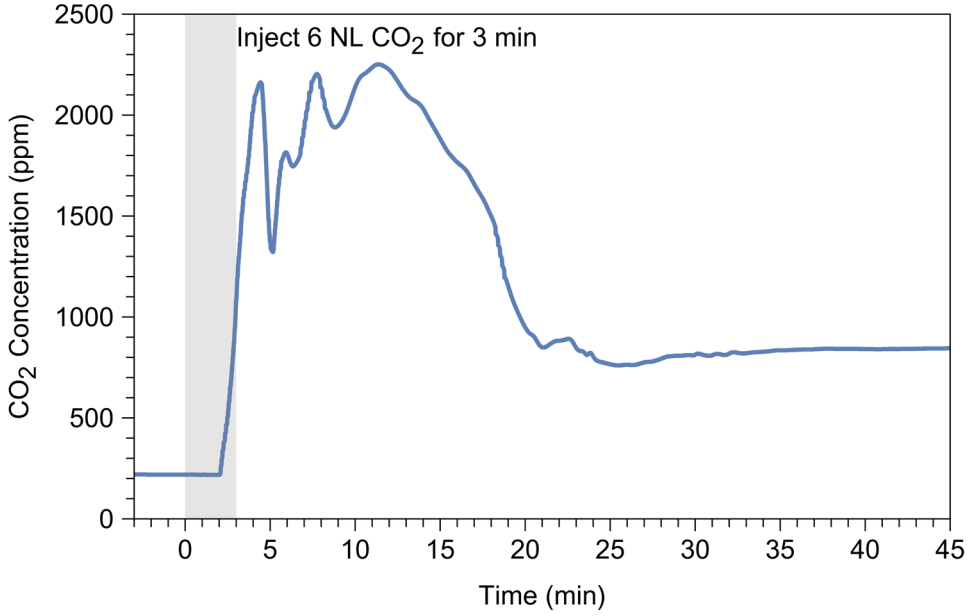

Figure S1. Time series of CO_2 concentration in the Teflon chamber for the experiment of testing the chamber volume. 6 NL (normal condition volume, at 273.15 K) of CO_2 was injected during the first 3 mins (gray area in the figure). CO_2 concentration was continuously measured by a CO_2 analyzer (SBA-5, PP System Inc.) at the opposite side of the chamber. The bag volume was determined to be 990 L at room temperature by the change in the CO_2 concentration. The measured volume was used in data analysis. The time scale for the complete mixing of CO_2 was approximately 30 mins.

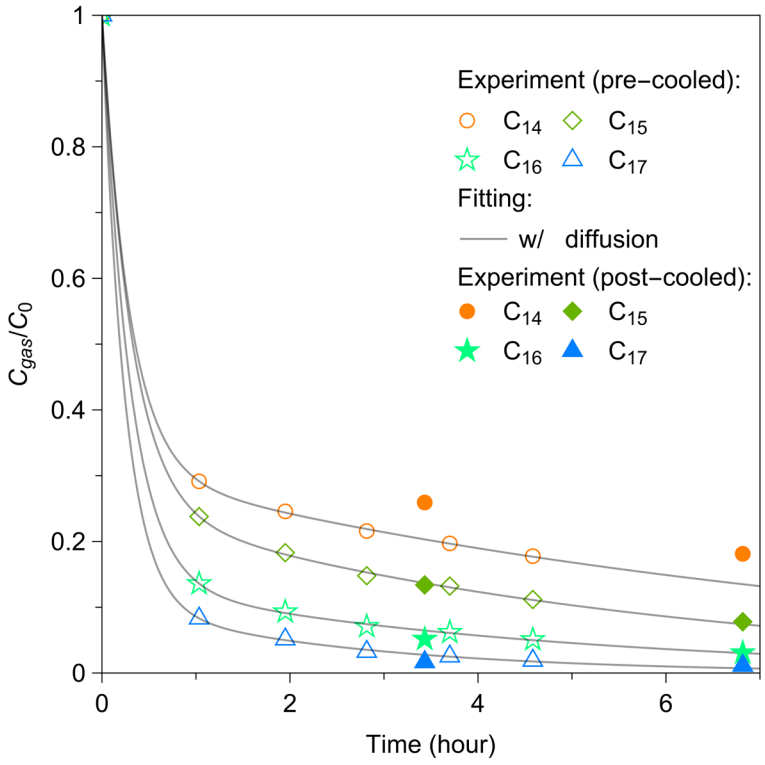

Figure S2. Comparison of C_{gas}/C_0 between pre-cooled experiment at 270 K (hollow points) and post-cooled experiment at 270.2 K (solid points). The two-layer kinetic sorption model was employed to fit the pre-cooled chamber data (black solid lines). Results in post-cooled experiments (solid points) align well with the two-layer kinetic model fitting results of pre-cooled experiment (black lines). The consistency between pre- and post- cooled experiment demonstrated the validity of employing post-cooled operation procedure.

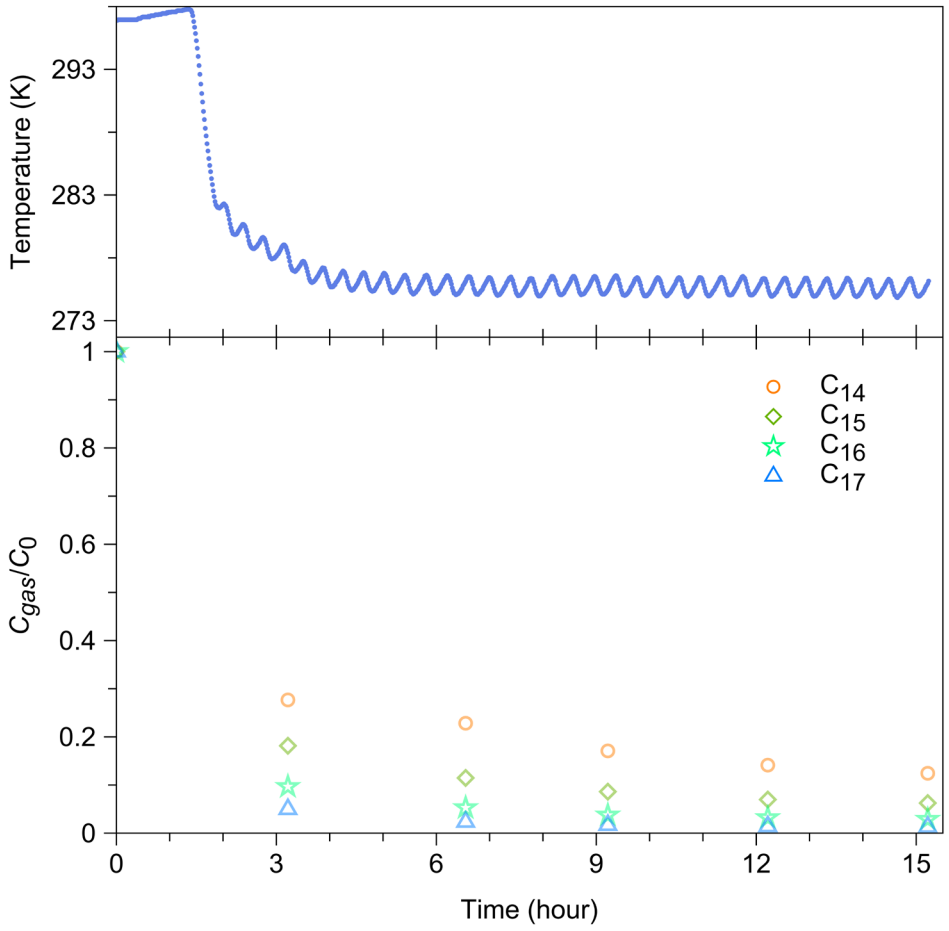

Figure S3. The values of C_{gas}/C_0 for C_{14}-C_{17} *n*-alkanes measured in the gas phase for the experiment at 275.7 ± 0.5 K. The freezer was turned on 1 hour after the completion of the injection.

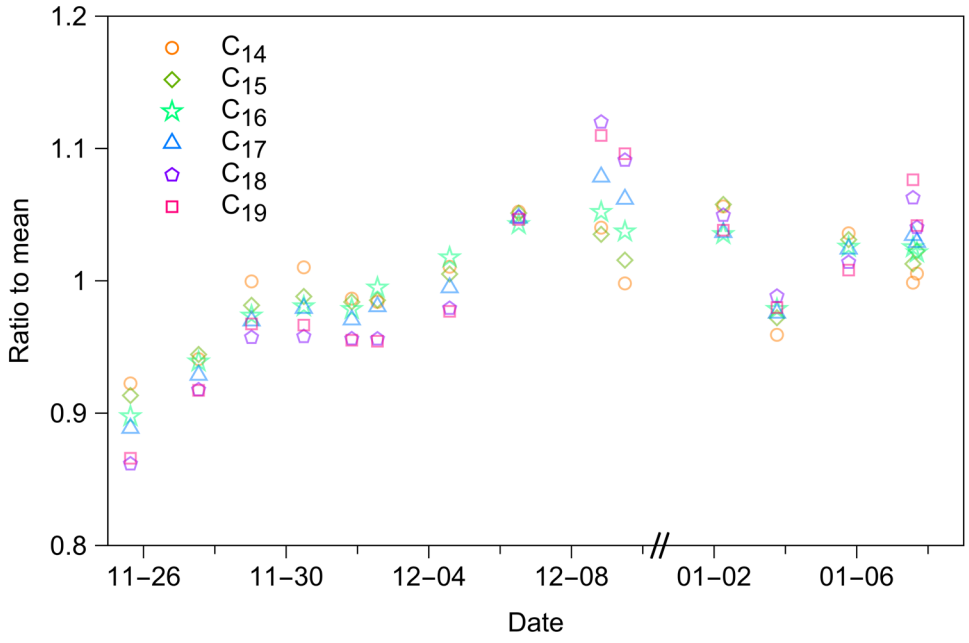

Figure S4. Relative changes in the signals of the *n*-alkanes standards during the experiment period. The data suggest that the sensitivity of the SV-TAG was stable within the fluctuation of ±10%.

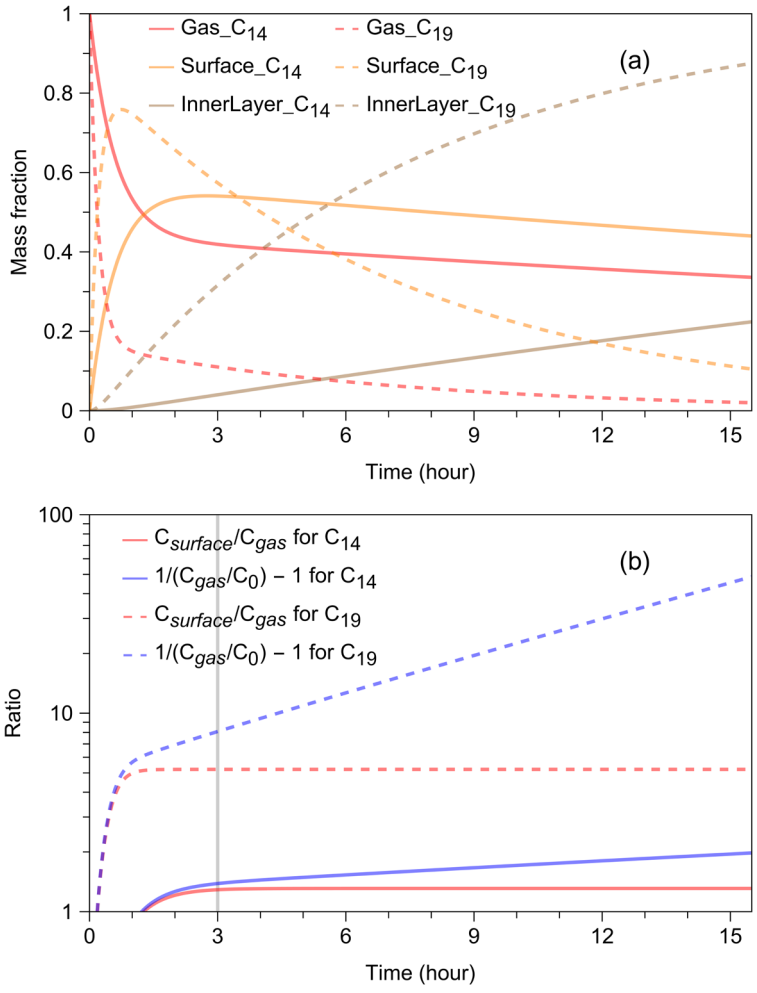

Figure S5. Simulation results of the two-layer model for room temperature experiment (Figure 3). (a) Time series of mass fraction of the total injection in gas, surface, and inner layer phases for C_{14} and C_{19} *n*-alkanes. Solid and dashed lines represent C_{14} and C_{19} *n*-alkanes respectively. Red, orange, and brown lines represent mass fractions in gas, surface, and inner layer phases respectively. (b) Time series of the ratio of mass in surface and gas phase ($C_{surface}/C_{gas}$) and the ratio of mass not in and in the gas phase ($1/[C_{gas}/C_0] - 1$) for C_{14} and C_{19} *n*-alkanes. Solid and dashed lines represent C_{14} and C_{19} *n*-alkanes respectively. Red and blue lines represent the values of $C_{surface}/C_{gas}$ and $1/[C_{gas}/C_0] - 1$ respectively. The gray solid line indicates 3 hours as we choose the 3-hour measurements $(1/[C_{gas}/C_0]_{\text{at 3 hours}} - 1)$ to approximate K_{eq} in the main text.

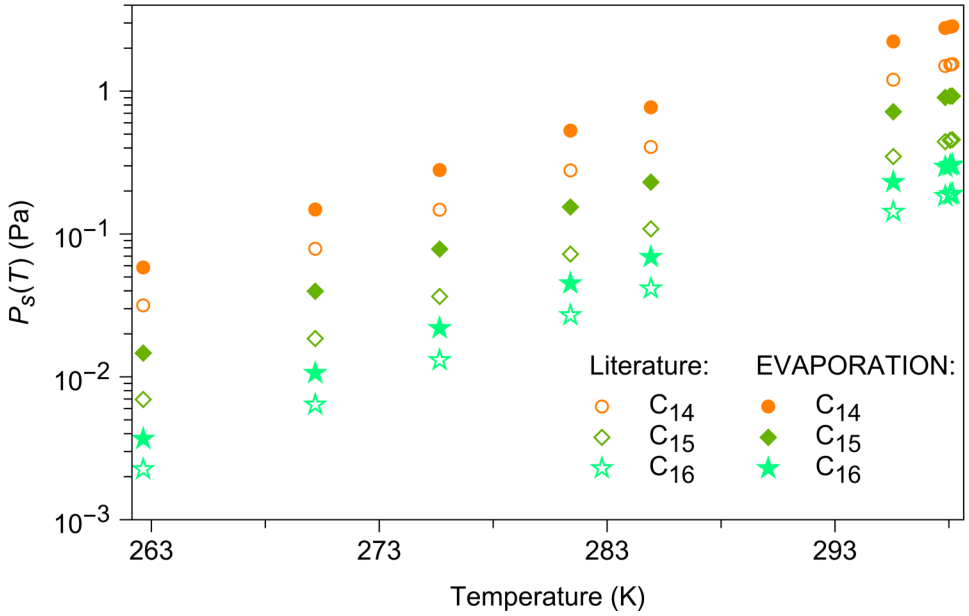

Figure S6. Saturation vapor pressures at different experimental temperatures for C_{14}-C_{16} *n*-alkanes calculated by the EVAPORATION method (Compernolle et al., 2011) and the Clausius–Clapeyron equation with literature values (Fitzpatrick, 2004; Rumble, 2022).

Text S1. Uncertainty in approximating K_{eq} as $1/[C_{gas}/C_0]_{\text{at 3 hours}} - 1$.

The uncertainties in approximating K_{eq} as $1/[C_{gas}/C_0]_{\text{at 3 hours}} - 1$ were estimated in two ways. First, the fitting parameters for room-temperature experiment in Figure 3 were used to simulate the kinetic process of wall loss (Figure S5a). Specifically, the values of $C_{surface}/C_{gas}$ and $1/[C_{gas}/C_0] - 1$ for C_{14} and C_{19} *n*-alkanes were retrieved, which were shown as red and blue lines in Figure S5b. These two *n*-alkanes were chosen, as they represent the highest and lowest volatile species in the room-temperature experiment. For both *n*-alkanes, $C_{surface}/C_{gas}$ stabilized by 3 hours, suggesting gas-surface partitioning reached equilibrium. In other words, K_{eq} equals to $C_{surface}/C_{gas}$ at 3 hours. The discrepancy between the red lines and corresponding blue lines at 3 hours in Figure S5b was thus the bias caused by approximating K_{eq} as $1/[C_{gas}/C_0]_{\text{at 3 hours}} - 1$. For C_{14} and C_{19} *n*-alkanes, this approximation overestimated the values of K_{eq} by 7% and 55%, respectively.

The uncertainties were also estimated by the room-temperature experimental results. Since no temperature controlling process was needed for room temperature experiments, the experimental data can be fitted using the two-layer model. Values of k_1 and k_{-1}, and thus K_{eq} (=k_1/k_{-1}) can be obtained. Three sets of experiments were conducted at room temperature, which allows for estimating the experimental uncertainties as standard deviations among these replicated runs. As shown in Table S3, values of K_{eq} and $1/[C_{gas}/C_0]_{\text{at 3 hours}} - 1$ agree well within experimental uncertainties. On average, this approximation overestimates K_{eq} by 22%, which would not influence our main results.

In summary, although the model simulation implies potentially large uncertainties, the comparison based on experimental data demonstrates the validity of the approximation.

Reference

Compernolle, S., Ceulemans, K., and Muller, J. F.: EVAPORATION: A new vapour pressure estimation method for organic molecules including non-additivity and intramolecular interactions, Atmos. Chem. Phys., 11, 9431-9450, https://doi.org/10.5194/acp-11-9431-2011, 2011.

Fitzpatrick, R. B.: Haz-Map: information on hazardous chemicals and occupational diseases, Med. Ref. Services Quart., 23, 49-56, https://doi.org/10.1300/J115v23n02_05, 2004.

Krechmer, J. E., Pagonis, D., Ziemann, P. J., and Jimenez, J. L.: Quantification of gas-wall partitioning in Teflon environmental chambers using rapid bursts of low-volatility oxidized species generated in situ, Environ. Sci. Technol., 50, 5757-5765, https://doi.org/10.1021/acs.est.6b00606, 2016.

Matsunaga, A. and Ziemann, P. J.: Gas-wall partitioning of organic compounds in a Teflon film chamber and potential effects on reaction product and aerosol yield measurements, Aerosol Sci. Technol., 44, 881-892, https://doi.org/10.1080/02786826.2010.501044, 2010.

Rumble, J.: CRC handbook of chemistry and physics, CRC press, ISBN978-1032121710, 2022.

Yeh, G. K. and Ziemann, P. J.: Alkyl nitrate formation from the reactions of C_8-C_{14} n-alkanes with OH radicals in the presence of NO_x: Measured yields with essential corrections for gas-wall partitioning, J. Phys. Chem. A, 118, 8147-8157, https://doi.org/10.1021/jp500631v, 2014.

Yeh, G. K. and Ziemann, P. J.: Gas-wall partitioning of oxygenated organic compounds: Measurements, structure-activity relationships, and correlation with gas chromatographic retention factor, Aerosol Sci. Technol., 49, 726-737, https://doi.org/10.1080/02786826.2015.1068427, 2015.